Textile & Leather Review

ISSN 2623-6281 | www.tlr-journal.com | 10.31881/TLR

Comparison of Structural and Thermal Properties of *Bauhinia Vahlii* Fibre Extracted with Varied NaOH Concentrations

Goutam Bar, Kavita Chaudhary

How to cite: Bar G, Chaudhary K. Comparison of Structural and Thermal Properties of *Bauhinia Vahlii* Fibre Extracted with Varied NaOH Concentrations. Textile & Leather Review. 2023; 6:151-166. https://doi.org/10.31881/TLR.2023.027

How to link: https://doi.org/10.31881/TLR.2023.027

Published: 26 April 2023

Comparison of Structural and Thermal Properties of *Bauhinia Vahlii* Fibre Extracted with Varied NaOH Concentrations

Goutam BAR[1,2*], Kavita CHAUDHARY[1]

[1]Department of Design, Banasthali Vidyapith, Banasthali, Rajasthan, India

[2]Department of Textile Design, National Institute of Fashion Technology, Bhubaneswar, India

[*]goutam.bar@nift.ac.in

Article

https://doi.org/10.31881/TLR.2023.027

Received 11 March 2023; Accepted 20 April 2023; Published 26 April 2023

ABSTRACT

Plant-based natural fibres have great potential to replace synthetic materials. They come from renewable resources and are biodegradable. The physical, structural, and thermal properties of lignocellulosic fibres can be slightly modified by adopting various fibre extraction methods and chemical treatments. This research aims to compare the structural and thermal properties of Bauhinia vahlii fibres (BVFs) extracted by the different extraction processes. The Bauhinia vahlii bark was treated with 10% (w/w) and 15% (w/w) NaOH solution at 95°C for two hours, followed by mechanical and manual extraction and comparison of the structural and thermal properties. Bauhinia vahlii fibres extracted with 15% NaOH solution (BVFs15) have higher crystallinity and more surface roughness than fibres extracted with 10% NaOH (BVFs10). Thermal analysis indicates that the maximum thermal degradation temperature and kinetic activation energy are slightly higher for Bauhinia vahlii fibres extracted with a 15% NaOH solution. The BVFs15 has improved structural and thermal properties and can be used for natural yarn manufacture.

KEYWORDS

Bauhinia vahlii, FTIR, morphological characterization, thermal analysis, X-ray diffraction, alkaline treatment

INTRODUCTION

Production and usage of synthetic textile materials have increased in the last few decades for their durability and low cost. However, these synthetic materials are non-biodegradable, may not be suitable for certain skin conditions, and are less comfortable than natural fibres. Moreover, the disposal of these non-biodegradable synthetic materials creates landfill and pollutes the environment [1,2]. Consumers are looking for bio-based sustainable textile materials for conventional textiles in this current context. Plant-based natural fibres have great potential to replace these synthetic materials as these fibres are biodegradable, environment friendly, and come from renewable resources [3]. Many plant fibres have been already explored for usage in natural fibre-reinforced composite materials. There is limited literature on the extraction of textile-grade plant-based natural fibres. In this research, an attempt is made to obtain textile-grade fibres from the *Bauhinia vahlii* plant bark.

Bauhinia vahlii plant bark is known as an excellent source of vegetable fibre [4]. It is a huge tropical climber and among the widespread Indian Bauhinia species belonging to the legume family, Angiospermae class, Fabales order. The image of the plant is shown in Figure 1. *Bauhinia vahlii* plant is commonly grown in the world's warmer climates, mainly in Asian, African, and South American countries [5,6]. This plant is found in India's central and eastern states as well as the lower Himalayan region. In the Hindi language, this plant is known as “Maloo Creeper” and in Odisha, famous by the name of “Siali”. The tribal people of Odisha prepare food plates from the leaves and simple household items from the stem bark of this plant for their livelihood [5]. Leaf and bark extract of the *Bauhinia vahlii* plant is used in traditional medicine to treat diabetes, inflammation, pain, etc. based on its antioxidant and antimicrobial characteristics [7,8].

Figure 1. *Bauhinia vahlii* plant

There are several ways to extract the natural fibres or remove the gummy substances from the natural fibres like mechanical extraction, retting, and chemical treatments [9,10]. Decortication and post-decortication are the widely used mechanical extraction methods for lignocellulosic fibres. These fibres can also be extracted by water, dew, and enzymatic retting method. Chemical treatments include alkaline, acid, and emulsion treatment [9,11]. Alkaline treatment separates the fibres and increases the surface area for dye penetration [12]. Alkaline treatment also modifies the surface by removing a significant amount of lignin, hemicellulose, pectin, and oily substances from the fibre [13]. The degree of surface modification depends on the treatment time, temperature, and NaOH concentration. Alkaline treatment increases fibre density and crystallinity percentage by removing noncellulosic materials from the fibres [14,15].

This research aims to compare the structural and thermal characteristics of *Bauhinia vahlii* bark treated with 10% (w/w) and 15% (w/w) NaOH solution to understand the possibilities of application in textiles. Structural properties of *Bauhinia vahlii* fibres have been analysed using various methods, including surface morphology, cross-sectional imaging, X-ray analysis, and functional group identification using FTIR. Thermogravimetric analysis has also been carried out.

EXPERIMENTAL

Materials

Bauhinia vahlii plant bark was collected from the Simlipal forest, Odisha, India. Acetic acid and NaOH of Rankem, Maharashtra, India, are used for fibre extraction.

Fibre extraction method

Extraction of *Bauhinia vahlii* fibre from the bark involves several steps. Initially, collected *Bauhinia vahlii* barks were cut into 30 to 45 cm long slices to obtain *Bauhinia vahlii* bast fibre. The bark pieces were dipped in water for 24 hours at room temperature after being physically cleaned to separate the immature and woody contents. The softened bark samples were treated with a NaOH solution with different concentrations [10% and 15% (w/w)] separately at boiling temperature for 2 hours to remove the lignin and other impurities. Causticized bark samples were rinsed and passed through a mangle at 3 bar pressure to remove the gummy materials. After two rounds of squeezing, the material was washed for 30 minutes at 100 °C, followed by neutralization with acetic acid. Removal of any remaining gums was accomplished by scraping the bark with a regular knife. Fibre layers were split manually from the treated bark samples layer by layer. Fibre layers are stretched in width-wise directions and dried. The dried layers were cut into 5 cm lengths. The fibre strands were taken out in the width-wise direction. A hand carder further opened the extracted fibres, i.e., BVFs10 and BVFs15. The stepwise BVFs extraction process is illustrated in Figure 2.

Figure 2. The extraction method of BVFs10 and BVFs15 a) *Bauhinia vahlii* plant bark b) boiling with NaOH c) scraping of gummy substances d) fibre layers separation e) cutting of fibrous layers into shorter length f) fibre after manual extraction g) hand carding h) hand carded fibre

Morphological characterization of *Bauhinia vahlii* fibres

Surface characteristics and cross-sectional view of BVFs10 and BVFs15 were captured in an EVO 50, an SEM of Zeiss at varied magnification for morphological studies. For a cross-sectional view, a BVFs sample was prepared by inserting a bunch of fibre into a cork and finely slicing them with a cutter. A fine layer of gold plating was done to the fibre surface to prevent electrical charge build-up.

X-ray diffraction (XRD) analysis of *Bauhinia vahlii* fibres

The crystallinity of BVFs10 and BVFs15 was calculated utilizing the area under the curve method. For crystallinity index (CI) estimation, XRD analysis was done using X'pert PRO, an X-ray diffractometer of analytical with a 2 deg/min scanning rate. The wavelength of the X-ray was 0.154 nm. Chopped and ground BVFs powder was utilized for the characterization. The CI of BVFs10 and BVFs15 were calculated using the below equation [16].

$$\mathrm{CI} = \frac{\mathrm{A_{Crystalline}}}{\mathrm{A_{Total}}} \mathrm{x}\, 100 \qquad (1)$$

$A_{Crystalline}$ is the area under the crystalline peak region, and A_{Total} is the total area under the X-ray spectrum. OriginPro software was used to measure the area. The interplanar spacing of BVFs was calculated at different lattice planes using Bragg's equation [17].

$$n\lambda = 2d_{hkl}\sin\theta \quad (2)$$

Where λ is the X-ray wavelength, d_{hkl} denotes the interplanar distance of hkl crystallographic planes, θ indicates Bragg's angle, and n denotes the diffraction order. Generally, n equals 1 for the most intense diffraction peak. The crystallite size (CS) of BVFs10 and BVFs15 was computed by Scherrer's equation [18].

$$CS = \frac{K\lambda}{\beta\cos\theta} \quad (3)$$

Where K stands for Scherrer's constant (0.89), β denotes the peak's full width at half-maximum (FWHM) in radian.

Fourier Transform Infrared Analysis

FTIR spectra of the BVFs10 and BVFs15 were obtained in a Nicolet iS-50 Thermo FTIR from 400 to 4000 cm^{-1} wavenumber using the potassium bromide pellet method to identify the functional group. A potassium bromide pellet was made by blending and compacting the finely ground BVFs powder with potassium bromide in a 1:9 ratio. A potassium bromide pallet was prepared for BVFs10 as well as BVFs15.

Thermogravimetric Analysis

Thermal analysis of BVFs10 and BVFs15 was performed using the Simultaneous thermal analyser SDT650. In a thermogravimetric study, the thermal stability of the fibre is analysed, where a small amount of fibre sample is kept inside a programmed temperature-controlled enclosure. The instrument measures the weight of the left-over sample very accurately as a function of time and temperature. The scanning continued from 25 °C to 750 °C in a nitrogen atmosphere having a heating rate of 10 °C/min. Using Origin Pro software, the obtained data were used to plot thermogravimetric and differential thermogravimetric. The kinetic activation energy (E_a) of BVFs10 and BVFs15 was computed using Broido's equation [19].

$$ln\left[ln\left(\frac{1}{y}\right)\right] = -\left(\frac{E_a}{R}\right)\left[\left(\frac{1}{T}\right) + K\right] \quad (4)$$

Where y, R, T, and K are the normalized weight, gas constant, temperature in kelvin, and reaction rate constant, respectively.

RESULTS AND DISCUSSION

Morphological Characteristics of Bauhinia Vahlii Fibre

The SEM images of BVFs extracted with 10% and 15% NaOH are shown in Figure 3, at 1000X. It can be observed in Figure 3(a) that the fibres are not adequately separated when they are extracted with a 10% NaOH solution. The lack of separation is likely due to the lignin and wax, which tend to act as cementing material [13,20]. In Figure 3(b) separation of fibres is visible. This fibre separation states that a significant quantity of lignin and waxes are removed from the fibre structure when *Bauhinia vahlii* bark is treated with a 15% NaOH solution [13]. It can also be observed in Figure 4(a) that the surface of the BVFs is smoother with several lumps of impurities in the case of fibre extracted with 10% NaOH solution. The Causticizing process with 15% NaOH hydrolysed the hemicellulose and removed a significant quantity of lignin and pectin from the *Bauhinia vahlii* bark, which made the fibre surface rougher [21]. Figure 4(b) shows surface roughness and a few fragmented impurities on the fibre surface. Fibre roughness reduces the slippage between the fibres in the yarn due to better mechanical interlocking and enhances the yarn's tensile properties [22]. Figures 5(a) and 5(b) shows the cross-sectional view of the BVFs extracted with 10% and 15% NaOH, respectively. The cross-sectional view of BVFs10 is very much irregular in shape in contrast to BVFs15. Fibres' cross-sections range from circular to flat oval in the case of BVFs15. Few BVFs15 samples have an eye-shaped lumen.

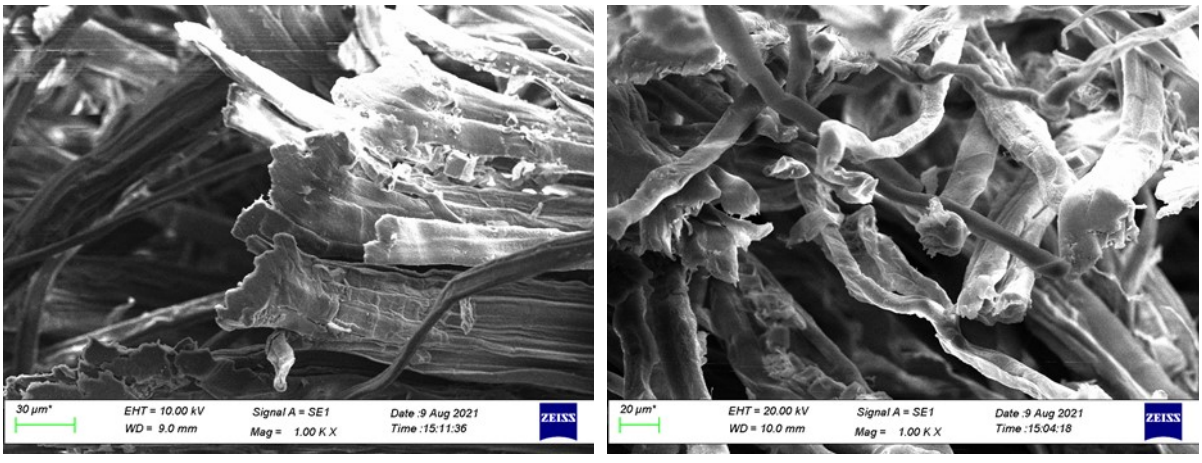

a) b)

Figure 3. SEM images of opened fibres a) BVFs10 b) BVFs15 at 1000X magnification

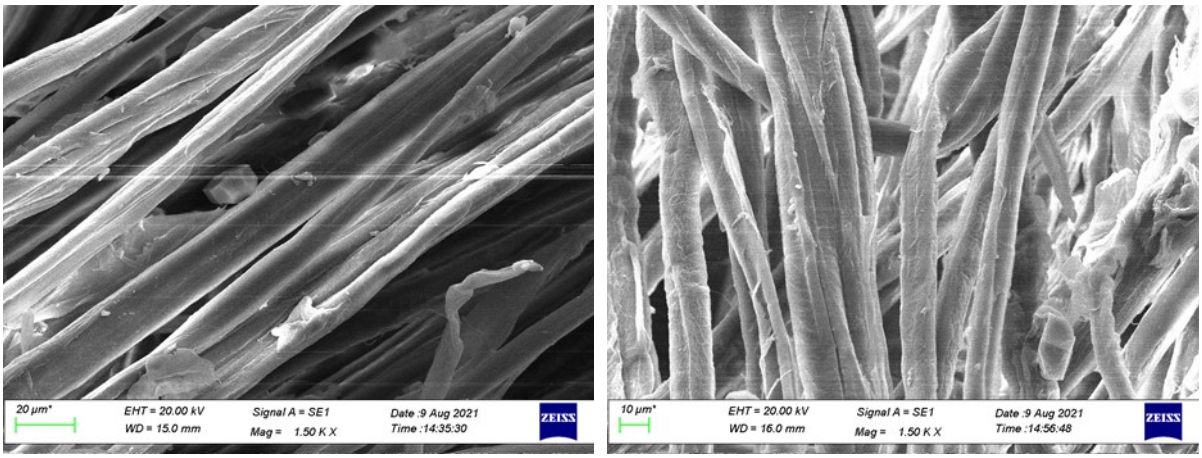

a) b)

Figure 4. Longitudinal view of a) BVFs10 b) BVFs15 at 1500X magnification

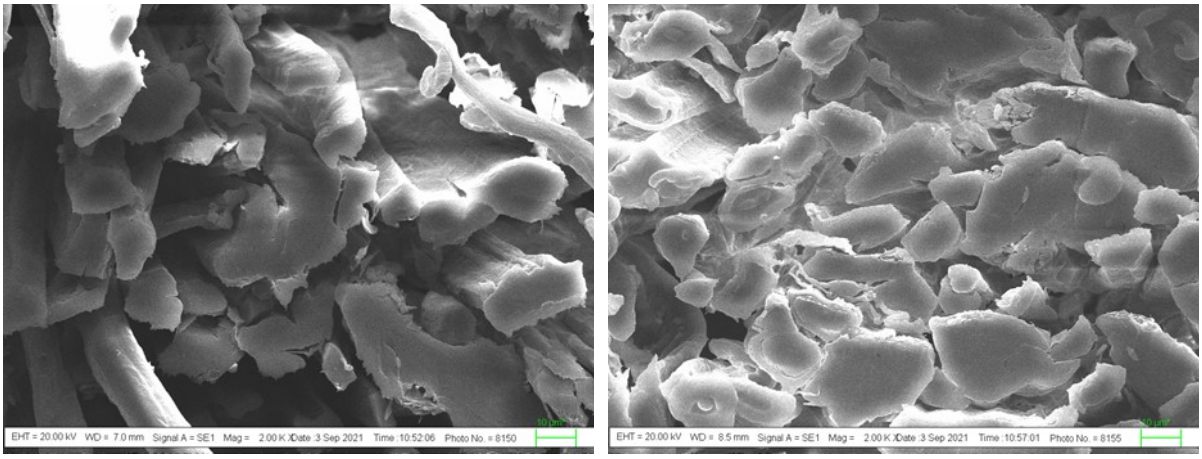

a) b)

Figure 5. Cross-sectional view of a) BVFs10 b) BVFs15 at 2000X magnification

FTIR Analysis of *Bauhinia Vahlii* Fibre

The FTIR spectrum of BVFs extracted with 10% NaOH, illustrated in Figure 6(a), helps to identify its functional groups. The characteristic peak at 3342, 2900, 1645, 1428, and 1369 cm^{-1} wavenumbers confirm the presence of cellulose in BVFs [23-26]. The presence of hemicellulose in BVFs10 is verified by the appearance of distinctive peaks at 2900, 1204, 1162, and 897 cm^{-1} wavenumbers [25,26]. The characteristic peaks at 1110, 1060, and 1036 cm^{-1} wavenumbers confirm the presence of lignin in BVFs [25,27]. Figure 6(b) illustrates the FTIR absorbance spectrum of BVFs extracted with 10% and 15% NaOH. It is clear from the FTIR spectrum that neither any new peak was found nor any significant shift of peaks was observed in the case of BVFs extracted with 15% NaOH compared with the fibre extracted with 10% NaOH. Only an increase in absorbance peak intensities was noticed in the case of BVFs15 compared to BVFs10. Such an increase in absorbance peak intensities indicates the increase in surface

roughness of the BVFs due to higher concentration alkaline treatment to the *Bauhinia vahlii* plant bark [28,29]. Hydrolysis of hemicellulose caused surface roughness due to treatment with a 15% NaOH solution [21]. An increase in surface roughness is also evident in the longitudinal view of BVFs15 in Figure 4(b). According to the FTIR spectra of BVFs, the fibre contains cellulose, hemicellulose, and lignin. Peak positions and functional group allocation of BVFs10 and BVFs15 are tabulated in Table 1.

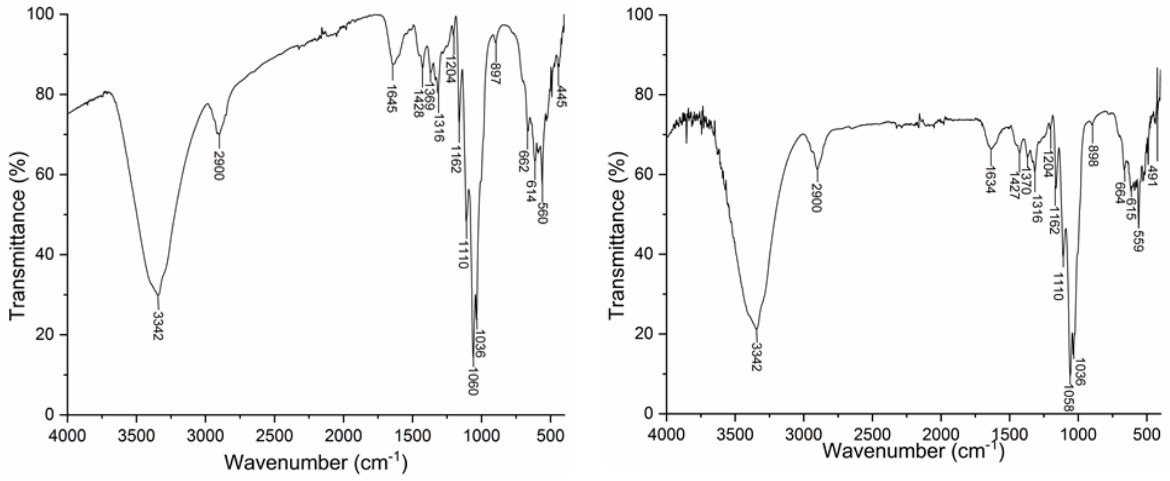

a) b)

Figure 6. Fourier transform-infrared analysis of a) BVFs10 b) BVFs15

Table 1. Peak positions and functional group allocation of BVFs10 and BVFs15

Wavenumber(cm^{-1})		Functional group allocation	Fibre component	References
BVFs10	BVFs15			
3342	3342	O-H bond stretching	α-cellulose	[23,26]
2900	2900	Stretching vibration of the C-H bond	Cellulose and hemicellulose	[26]
1645	1634	Vibration of absorbed water and C=O stretching	Cellulose and lignin	[23,24]
1428	1427	CH_2 symmetric bending	Cellulose	[30]
1369	1370	-CH bending vibration	Cellulose	[25]
1316	1316	C-O stretching of aromatic rings	Cellulose polysaccharides	[25]
1204	1204	-COO vibration of the acetyl group	Hemicellulose	[31]
1110	1110	In-plane deformation of aromatic C-H bond	Lignin	[25]
1060 & 1036	1058 & 1036	Symmetric C-O-H stretching	Lignin	[24,27]
1162 & 897	1162 & 898	C-O-C stretching at β-(1-4)-glycosidic linkages	Cellulose and hemicellulose	[25,32,33]

XRD Analysis of Bauhinia Vahlii Fibre

X-ray diffraction is a structural assessment technique based on the X-ray of a sample. It allows the determination of the microcrystalline as well as polycrystalline phases of fibres. Figure 7(a) shows an X-ray diffractogram of BVFs10. Two prominent diffraction peaks are visible in the X-ray diffraction pattern at 2θ near 14.95° and 22.85° corresponding to (101) and (002) crystal lattice plane, respectively [6]. The strong peak near 2θ = 22.85° indicates the lattice plane of cellulose I [6]. The presence of hemicellulose, lignin, and amorphous cellulose is confirmed by a broad peak around 2θ = 14.95° [33]. The crystalline region of BVFs10 is lying intermediate between 19.18° to 24.88° and 13.61° to 17.88°. The crystallinity index of BVFs10 is computed as 51.62%. Using Bragg's equation, both peaks' interplanar spacing of BVFs10 is determined as 0.59 and 0.39 nm. The crystallite size in (101) and (002) crystal lattice planes are 3.58 and 2.68 nm, correspondingly, with a mean value of 3.13 nm.

The X-ray diffraction pattern of BVFs15, as displayed in Figure 7(b), also has two major diffraction peaks like BVFs10 with higher peak intensities. Peaks occurred at 2θ near 15.23°, and 22.79° characterizes the presence of cellulose, hemicellulose, and lignin. The crystalline region of BVFs15 ranges from 19.65° to 25.21° and 13.17° to 17.97°. The CI of BVFs15 is 56%. The CI increases by 4.38% owing to the removal of hemicellulose and lignin from the fibre and an overall increase in cellulose percentage. The interplanar spacing of BVFs15 in the above-mentioned peaks is 0.58 nm and 0.39 nm. The crystallite size (CS) in (1 0 1) and (0 0 2) crystal lattice planes are 3.84 and 2.56 nm, correspondingly, with a mean CS of 3.2 nm. The crystallinity index of BVFs10 and BVFs15 are very similar to those of other plant-based natural fibres like jute, ramie, and purple bauhinia [6]. The mean CS of BVFs10 and BVFs15 is close to the other cellulosic natural fibres like flax, jute, and Acacia nilotica L. and smaller than cotton [6].

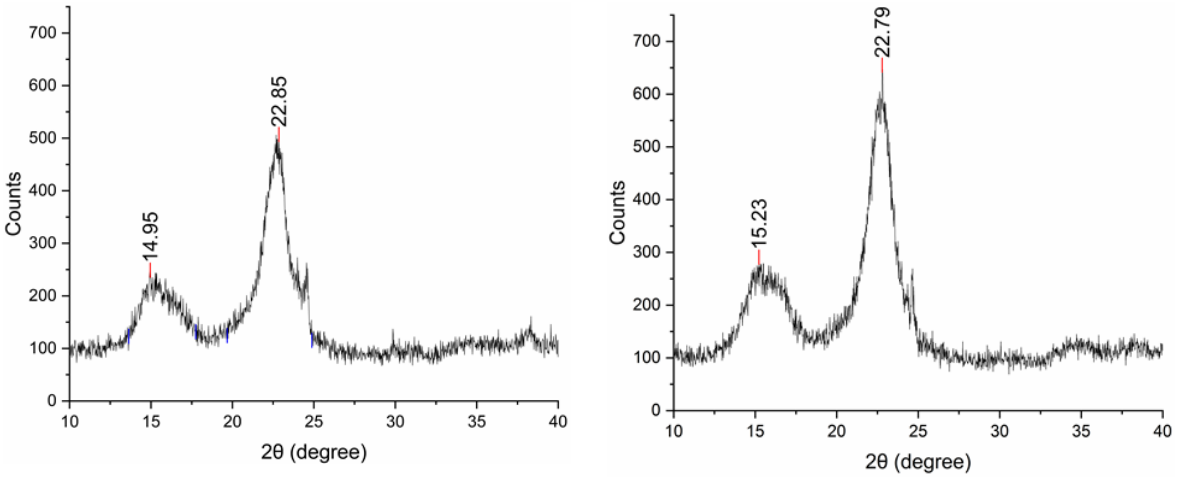

a) b)

Figure 7. X-ray diffractogram of a) BVFs10 b) BVFs15

Thermal Analysis of Bauhinia Vahlii Fibre

The thermal stability analysis of lignocellulosic fibre for conventional or technical textiles is of paramount importance. The knowledge of the thermal characteristics of fibres helps to predict the safe processing temperature, which is analysed using their thermogravimetric (TG) and derivative thermogravimetric (DTG) curves. Figure 8(a) illustrates the TG and DTG graph of BVFs10. As it is evident from the figure, BVFs10 loses weight through multiple phases of degradation as the temperature increases. Two endothermal peaks are noticed in the first phase of degradation around 75 °C and 165 °C in the DTG curve. The endothermic peak at 75 °C is related to the physical desorption of water present in fibre in the form of moisture. The second one at 165 °C is linked to the thermal dehydration of structurally bound water within the fibre [34]. Till 168 °C, a 9.4% weight loss is observed, with a total weight loss of 10.21% in the first degradation phase up to 231 °C and thermally stable up to this temperature. The second phase of degradation begins at 231 °C, as seen in the shoulder region of the DTG curve, which is linked to the disintegration of hemicellulose [34]. Above 300 °C, a higher rate of decomposition is observed with a very deep endothermic peak at 364 °C, associated with the degradation of residual hemicellulose, α-cellulose, and glycosidic bonds of cellulose [35]. Cellulose is a long-chain polymer structure without branches, has higher thermal stability than hemicellulose, and degrades later [34]. This degradation phase continued to 398 °C with a weight loss of 58.21%. The degree of decomposition is decreased in the third degradation phase as maximum cellulose pyrolysis in the second stage. This phase is linked to the decomposition of the fibre's remaining cellulose, lignin, and aromatic compounds [36]. Lignin is full of aromatic rings with many functional groups with different thermal stabilities and decomposes slowly through a wider range of temperatures than cellulose and hemicellulose [34,37]. This phase continued to 725 °C with an endothermal peak near 491 °C linked to the maximum degradation of lignin [27]. A weight loss of 15.31% was noticed in this phase, and 16.27% char content was recorded at 750 °C.

BVFs15 shows similar thermal behaviour to BVFs10, as seen in Figure 8(b). The first stage of decomposition shows two endothermal peaks at 59 °C and 151 °C having a total weight loss of 10.38%. Compared to BVFs10, both the peaks arose at approximately 15 °C lower temperature with a higher weight loss at the initial 100 °C, as evident in the figure. The surface roughness of BVFs15 enhances the moisture evaporation process and increases the rate of weight loss [38]. It also requires less thermal energy for moisture evaporation as a rough fibre surface facilitates it. A comparatively wider thermally stable zone from 159 °C to 233 °C is observed in BVFs15. In the second phase, 62.05% weight loss is observed owing to the degradation of hemicellulose, α-cellulose, and glycosidic bonds of cellulose. The maximum thermal degradation temperature is increased by 4 °C compared to BVFs10 due to the higher crystallinity of BVFs15 [39]. Moreover, lower crystallinity of BVFs10 increases the

extractive content in the fibre, which accelerates the thermal degradation process [34]. A weight loss of 11.92% is observed in the third phase, linked to the degradation of lignin and aromatic compounds. Compared to BVFs10, weight loss in the third phase is less due to less lignin in BVFs15. A higher concentration of NaOH removes lignin from BVFs15. At 750 °C, 16.27% char content was noticed.

To initiate the degradation of a material at a specific temperature, the minimal energy required is termed the kinetic activation energy of that material. 85.13 and 96.18 KJ/mol are the kinetic activation energy of BVFs10 and BVFs15, respectively, as calculated using Broido's plot illustrated in figures 9(a) and 9(b). The higher the kinetic activation energy required, the higher the decomposition temperature, as evident in DTG curves in figures 8(a) and 8(b).

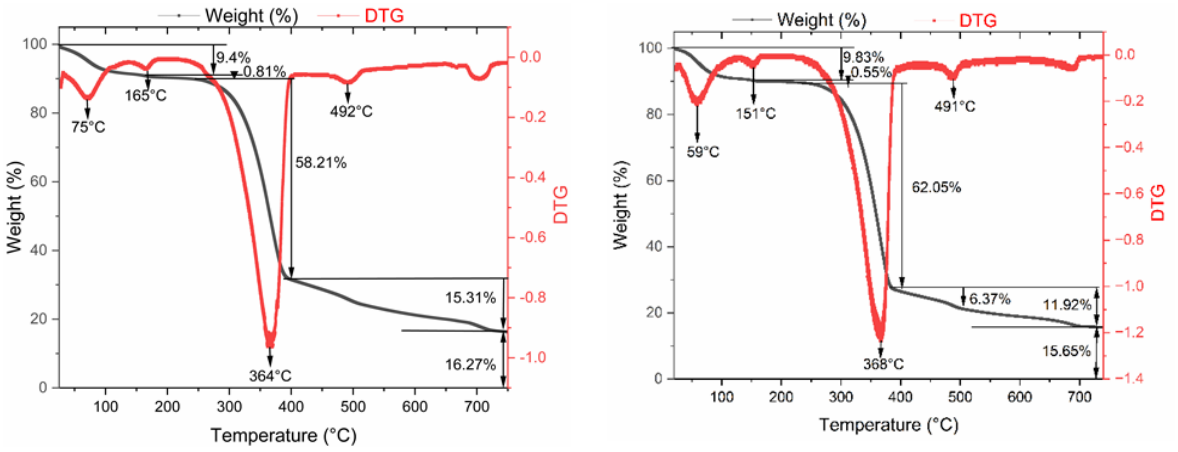

a) b)

Figure 8. Thermogravimetric and derivative thermogravimetric curve of a) BVFs10 b) BVFs15

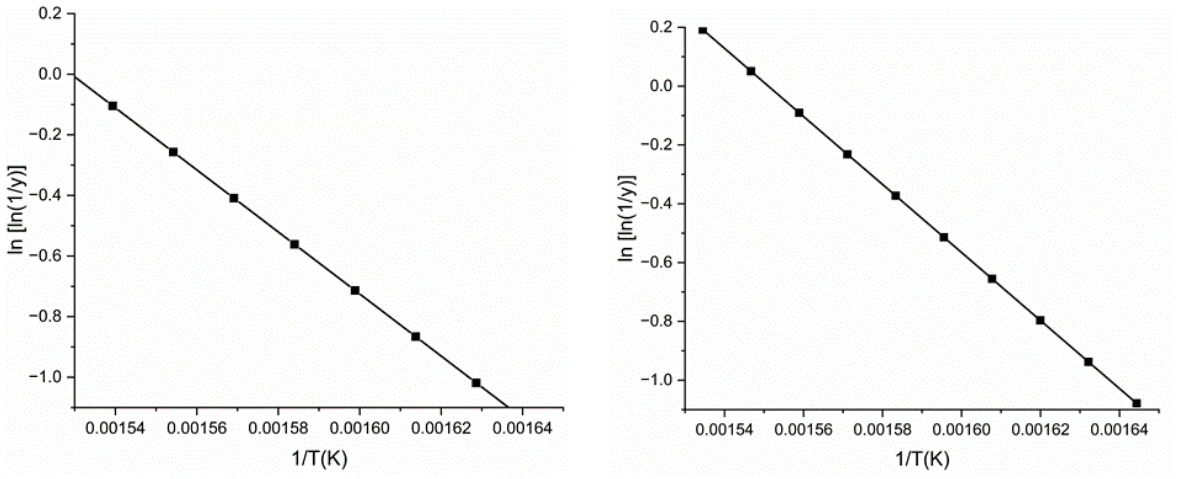

a) b)

Figure 9. Broido's plot of a) BVFs10 b) BVFs15

CONCLUSION

Bauhinia vahlii bark fibre extracted by treating with 15% NaOH solution has better fibre-to-fibre separation compared to BVFs extracted with 10% NaOH solution. Separating individual fibres is a prime prerequisite for converting these fibres into yarn. Moreover, the rough surface of BVFs15 will improve the fibre-to-fibre cohesiveness and the mechanical interlocking of the fibres. X-ray analysis confirms that BVFs15 has higher crystallinity compared to BVFs10 owing to the removal of hemicellulose and lignin from the fibre. There is no significant change in interplanar spacing in both the lattice planes. The CS of BVFs15 in (002) crystal lattice plane is slightly smaller compared to BVFs10. Thermogravimetric analysis reveals that BVFs15 have slightly better thermal stability having a maximum degradation temperature of 368 °C. The kinetic activation energies of BVFs10 and BVFs15 are 85.13 and 96.18 KJ/mol, respectively. Outcomes of all the studies suggest that BVFs15 has improved structural and thermal properties and can be used to manufacture natural yarn.

Author Contributions

Conceptualization – Bar G and Chaudhary K; methodology – Bar G; formal analysis – Bar G; investigation – Bar G; resources – Bar G; writing-original draft preparation – Bar G; writing-review and editing – Bar G and Chaudhary K; visualization – Bar G and Chaudhary K; supervision – Bar G and Chaudhary K. Both the authors have read and agreed to the published version of the manuscript.

Conflicts of Interest

The authors declare no conflict of interest.

Acknowledgements

The authors would like to acknowledge the support of the Central research facility, IIT, Delhi, India.

Funding

This research received no external funding.

REFERENCES

[1] Stone C, Windsor FM, Munday M, Durance I. Natural or synthetic – how global trends in textile usage threaten freshwater environments. Science of The Total Environment. 2020; 718:134689. https://doi.org/10.1016/j.scitotenv.2019.134689

[2] Ramasamy R, Subramanian RB. Synthetic textile and microfiber pollution: a review on mitigation strategies. Environmental Science and Pollution Research. 2021; 28:41596-41611. https://doi.org/10.1007/s11356-021-14763-z

[3] Singha AS, Rana AK. Preparation and characterization of graft copolymerized Cannabis indica L. fiber-reinforced unsaturated polyester matrix-based biocomposites. Journal of Reinforced Plastics and Composites. 2012; 31(22):1538-1553. https://doi.org/10.1177/0731684412442989

[4] Sahu SC, Pattanaik SK, Dash SS, Dhal NK. Fibre yielding plant resources of Odisha and traditional fibre preparation knowledge- An overview. Indian Journal of Natural Products and Resources. 2013: 4(4):339-347.

[5] Bar G, Bar M. Dyeing and flame-retardant finishing of silk fabric: an ecofriendly approach. SN Applied Sciences. 2020; 2:363. https://doi.org/10.1007/s42452-020-2114-8

[6] Bar G, Chaudhary K. Characterization of Textile Grade Novel *Bauhinia Vahlii* Fiber. Journal of Natural Fibers. 2023; 20(1):2143464. https://doi.org/10.1080/15440478.2022.2143464

[7] Dugasani S, Balijepalli MK, Tandra S, Pichika MR. Antimicrobial activity of *Bauhinia tomentosa* and *Bauhinia vahlii* roots. Pharmacognosy Magazine. 2010; 6(23):204-207. http://dx.doi.org/10.4103/0973-1296.66937

[8] Das SN, Jagannath PV, Dinda SC. Evaluation of anti–Inflammatory, anti–diabetic activity of Indian *Bauhinia vahlii (stembark)*. Asian Pacific Journal of Tropical Biomedicine. 2010; 2(3):S1382–S1387. https://doi.org/10.1016/S2221-1691(12)60421-3

[9] Lee CH, Khalina A, Lee SH, Liu M. A Comprehensive Review on Bast Fibre Retting Process for Optimal Performance in Fibre-Reinforced Polymer Composites. Advances in Materials Science and Engineering. 2020; 6074063. https://doi.org/10.1155/2020/6074063

[10] Rana AK, Thakur VK. The bright side of cellulosic hibiscus sabdariffa fibres: towards sustainable materials from the macro- to nano- scale. Materials Advances. 2021; 2(15):4945-4965. https://doi.org/10.1039/D1MA00429H

[11] Kale RD, Alemayehu TG, Gorade VG. Extraction and characterization of lignocellulosic fibers from *Girardinia Bullosa (Steudel) Wedd.* (Ethiopian Kusha Plant). Journal of Natural Fibers. 2020; 17(6):906-920. https://doi.org/10.1080/15440478.2018.1539940

[12] Ray D, Sarkar BK, Rana AK, Bose NR. Mechanical properties of vinyl polyester resin matrix composites reinforced with alkali-treated jute fibres. Composites Part A: Applied Science and Manufacturing. 2001; 32(1):119-127. https://doi.org/10.1016/S1359-835X(00)00101-9

[13] Kumar N, Das D. Alkali treatment on nettle fibers. The Journal of The Textile Institute. 2017; 108(8):1461-1467. https://doi.org/10.1080/00405000.2016.1257346

[14] Vardhini KJV, Murugan R, Selvi CT, Surjit R. Optimisation of alkali treatment of banana fibres on lignin removal. Indian Journal of Fibre & Textile Research. 2016; 41(2):156-160.

[15] Colom X, Carrillo F. Crystallinity changes in lyocell and viscose-type fibres by caustic treatment. European Polymer Journal. 2002; 38(11):2225-2230. https://doi.org/10.1016/S0014-3057(02)00132-5

[16] He J, Cui S, Wang S. Preparation and crystalline analysis of high-grade bamboo dissolving pulp for cellulose acetate. Journal of Applied Polymer Science. 2008; 107(2):1029-1038. https://doi.org/10.1002/app.27061

[17] Chiriac AI, Pastor FIJ, Popa VI, Aflori M, Ciolacu D. Changes of supramolecular cellulose structure and accessibility induced by the processive endoglucanase Cel9B from *Paenibacillus barcinonensis*. Cellulose. 2014; 21:203–219. https://doi.org/10.1007/s10570-013-0118-x

[18] Ahmed MJ, Balaji MA, Saravanakumar SS, Senthamaraikannan P. A comprehensive physical, chemical and morphological characterization of novel cellulosic fiber extracted from the stem of *Elettaria cardamomum* plant. Journal of Natural Fibers. 2021; 18(10):1460-1471. https://doi.org/10.1080/15440478.2019.1691121

[19] Md JS, Madhu S, Chakravarthy KS, Raju JSN. Characterization of Natural Cellulose Fibers from the Stem of *Albizia Julibrissin* as Reinforcement for Polymer Composites. Journal of Natural Fibers. 2022; 19(6):2204-2217. https://doi.org/10.1080/15440478.2020.1807440

[20] Patel U, Ray R, Mohapatra A, Das SN, Das HC. Effect of different chemical treatments on surface morphology, thermal and tensile strength of *Bauhinia vahlii* (BV) stem fibers. Journal of Natural Fibers. 2022; 19(1):280-291. https://doi.org/10.1080/15440478.2020.1739591

[21] Jayaramudu J, Guduri BR, Rajulu AV. Characterization of new natural cellulosic fabric *Grewia tilifolia*. Carbohydrate Polymers. 2010; 79(4):847-851. https://doi.org/10.1016/j.carbpol.2009.10.046

[22] Yao Y, Chen S. The effects of fiber's surface roughness on the mechanical properties of fiber-reinforced polymer composites. Journal of Composite Materials. 2013; 47(23):2909-2923. https://doi.org/10.1177/0021998312459871

[23] Hyness NRJ, Vignesh NJ, Senthamaraikannan P, Saravanakumar SS, Sanjay MR. Characterization of new natural cellulosic fiber from *Heteropogon contortus* plant. Journal of Natural Fibers. 2018; 15(1):146-153. https://doi.org/10.1080/15440478.2017.1321516

[24] Senthamaraikannan, P, Kathiresan M. Characterization of raw and alkali treated new natural cellulosic fiber from *Coccinia grandis.L*. Carbohydrate Polymers. 2018; 186:332-343. https://doi.org/10.1016/j.carbpol.2018.01.072

[25] Zhuang J, Li M, Pu Y, Ragauskas AJ, Yoo CG. Observation of potential contaminants in processed biomass using fourier transform infrared spectroscopy. Applied Sciences. 2020; 10(12):4345. https://doi.org/10.3390/app10124345

[26] Vijay R, Singaravelu DL, Vinod A, Sanjay MR, Siengchin S. Characterization of alkali-treated and untreated natural fibers from the stem of *Parthenium hysterophorus*. Journal of Natural Fibers. 2021; 18(1):80-90. https://doi.org/10.1080/15440478.2019.1612308

[27] Maheshwaran MV, Hyness NRJ, Senthamaraikannan P, Saravanakumar SS, Sanjay MR. Characterization of natural cellulosic fiber from *Epipremnum aureum* stem. Journal of Natural Fibers. 2018; 15(6):789-798. https://doi.org/10.1080/15440478.2017.1364205

[28] Gu X, Raghavan D, Nguyen T, VanLandingham MR, Yebassa D. Characterization of polyester degradation using tapping mode atomic force microscopy: exposure to alkaline solution at room temperature. Polymer Degradation and Stability. 2001; 74(1):139-149. https://doi.org/10.1016/S0141-3910(01)00138-0

[29] Li F, Xing Y, Ding X. Silica xerogel coating on the surface of natural and synthetic fabrics. Surface and Coatings Technology. 2008; 202(19):4721-4727. https://doi.org/10.1016/j.surfcoat.2008.04.048

[30] Manimaran P, Senthamaraikannan P, Muruganathan K, Sanjay MR. Physicochemical properties of new cellulosic fibers from *Azadirachta indica* plant. Journal of Natural Fibers. 2018; 15(1):29-38. https://doi.org/10.1080/15440478.2017.1302388

[31] Reddy KO, Reddy KRN, Zhang J, Zhang J, Rajulu AV. Effect of alkali treatment on the properties of Century fiber. Journal of Natural Fibers. 2013; 10(3):282-296. https://doi.org/10.1080/15440478.2013.800812

[32] Berglund J, D'Ortoli TA, Vilaplana F, Widmalm G, Wohlert-Bergenstrahle M, Lawoko M, Henriksson G, Lindström M, Wohlert J. A molecular dynamics study of the effect of glycosidic linkage type in the hemicellulose backbone on the molecular chain flexibility. The Plant Journal. 2016; 88(1):56-70. https://doi.org/10.1111/tpj.13259

[33] Baskaran PG, Kathiresan M, Senthamaraikannan P, Saravanakumar SS. Characterization of new natural cellulosic fibre from the bark of *Dichrostachys cinerea*. Journal of Natural Fibers. 2018; 15(1):62-68. https://doi.org/10.1080/15440478.2017.1304314

[34] Poletto M, Ornaghi Júnior HL, Zattera AJ. Reactions and Mechanisms in Thermal Analysis of Advanced Materials. In: Tiwari A, Raj B, editors. Reactions and Mechanisms in Thermal Analysis of Advanced Materials. Massachusetts: Scrivener Publishing LLC; 2015. p. 515-545. https://doi.org/10.1002/9781119117711.ch21

[35] Belouadah Z, Ati A, Rokbi M. Characterization of new natural cellulosic fiber from *Lygeum Spartum* L. Carbohydrate Polymers. 2015; 134(10):429-437. https://doi.org/10.1016/j.carbpol.2015.08.024

[36] Fiore V, Valenza A, Di Bella G. Artichoke (*Cynara cardunculus* L.) fibres as potential reinforcement of composite structures. Composites Science and Technology. 2011; 71(8):1138-1144. https://doi.org/10.1016/j.compscitech.2011.04.003

[37] Brebu M, Vasile C. Thermal Degradation of Lignin – A Review. Cellulose Chemistry and Technology. 2010; 44(9):353-363.

[38] Kieu HT, Zhou K, Law AWK. Surface morphology effect on the evaporation of water on graphene oxide: A molecular dynamics study. Applied Surface Science. 2019; 488:335-342. https://doi.org/10.1016/j.apsusc.2019.05.247

[39] Ouarhim W, Zari N, Bouhfid R, Qaiss A. Mechanical performance of natural fibers-based thermosetting composites. In: Jawaid M, Thariq M, Saba N, editors. Mechanical and Physical Testing of Biocomposites, Fibre-Reinforced Composites and Hybrid Composites. United Kingdom: Woodhead Publishing; 2019. p. 43-60. https://doi.org/10.1016/B978-0-08-102292-4.00003-5